Methods in Molecular Biology
DOI 10.1007/7651_2014_165

Patient-Specific Induced Pluripotent Stem Cell Models: Characterization of iPS Cell-Derived Cardiomyocytes

Toru Egashira, Shinsuke Yuasa, Shugo Tohyama, Yusuke Kuroda, Tomoyuki Suzuki, Tomohisa Seki, and Keiichi Fukuda

Abstract

Despite significant advances in medical treatment, cardiovascular disease is still a major cause of morbidity and mortality in advanced countries. To improve the outcome, the further promotion of basic cardiovascular science has a pivotal role for the developing novel therapeutic approach. However, due to the inaccessibility of human heart tissue, we couldn't obtain the sufficient amount of patient's heart tissues. The discovery of human-induced pluripotent stem cells (iPSCs) is highly expected to provide the breakthrough to this obstruction. Through the patient-specific iPSCs-derived cardiomyocytes, we could analyze the patient-specific heart diseases directly and repetitively. Herein we introduce the outline of creation for cardiac disease modeling using patient-specific iPSCs. Within several topics, we present the actual representative methodologies throughout the process from the derivation of cardiomyocytes to those of functional analysis.

Keywords: iPS cell, Cardiomyocyte, Purification, Electrophysiology

1 Introduction

In the mid of 2000s, the generation of induced pluripotent stem cells (iPSCs) brought a great impact on stem cell biology (1, 2). The major expected role of iPSCs could bear mainly consists of two parts, one is as a robust resource for the regenerative cell therapy and the other is as a tool for the creation of human genetic disease modeling. There are already many reports showing that iPSCs were generated from a variety of patients and those iPSC-derived differentiated cells successfully reproduced the disease phenotypes, and this type of analysis has shed light on the further understanding of the underlying disease mechanism and subsequently provided the cue for developing novel therapeutic approach (3). Along with the accumulation of individual research outcomes, the comprehensive research projects such as high-throughput drug screening by using patient-specific iPSC-derived cells have been designed, and actually some intriguing results are appealing (4–6). We have previously reported the disease modeling for long QT syndrome, a hereditary

arrhythmic disease with high incidence, by using patient-specific iPSCs (7). We clarified the molecular mechanism of the disease pathogenesis in the patient with novel KCNQ1 mutation and verified the appropriate medication through the drug response examination on electrical activity of the patient-specific iPSC-derived cardiomyocytes. Herein we introduce the outline how to examine the patient-specific iPSC-derived cardiomyocytes, which covers the whole process from the differentiation into cardiomyocytes from iPSCs to functional analyses.

2 Materials

2.1 Equipment

100 mm tissue culture dish (Falcon® 353003).

6-well tissue culture plate (Falcon® 353046).

24-well tissue culture plate (Falcon® 353047).

96-well tissue culture plate (Falcon® 353072).

Ultra-low attachment culture dishes, 100 mm petri dish (Corning® 3262).

15 ml conical tube (Falcon® 352096).

50 ml conical tube (Falcon® 352070).

1 ml plastic disposable pipette (Falcon® 357521).

2 ml plastic disposable pipette (Falcon® 357507).

5 ml plastic disposable pipette (Falcon® 357543).

10 ml plastic disposable pipette (Falcon® 357551).

25 ml plastic disposable pipette (Falcon® 357525).

50 ml plastic disposable pipette (Falcon® 357550).

20 μl filter tip (NIPPON Genetics® FGF-20S2).

200 μl filter tip (NIPPON Genetics® FGF-7032).

1,000 μl filter tip (NIPPON Genetics® FGF-10002).

Pasteur pipette (IWAKI® IK-PAS-9P).

0.22 μm pore size filter (Millipore®, SCGPT10RE).

40 μm cell strainer (Falcon® 352340).

100 μm cell strainer (Falcon® 352360).

40 μm cell strainer (Falcon® 352340).

Ultra-low attachment culture dishes, 100 mm petri dish (Corning® 3262).

Magnetic bar (IKAFLON® 1572000).

Magnetic stirrer (AS ONE® CS-1).

4-well chamber slide (Nunc® Lab-Tek®II 154534).

Micro cover glass (Matsunami Glass® C024501).

LSM510 Meta Confocal Microscope (ZEISS).

Multi-electrode array (MEA) chips.

Axopatch 200B (Molecular Devices).

Digidata 1440A (Molecular Devices).

pClamp software 10.2 (Molecular Devices).

Glass pipette (Harvard Apparatus).

Matsunami glass bottom dish (Matsunami).

Magnetic stirrer bar (AS ONE® CS-1).

35 mm glass-bottomed dish (IWAKI).

2.2 Materials

Collagenase, type IV, powder (GIBCO® 17104-019).

DMEM/F12 (Sigma-Aldrich® D6421).

1 mg/ml of collagenase, type IV solution: Dissolve 100 mg of collagenase IV in 100 ml of DMEM/F12 and through with a 0.22 μm pore filter. Aliquot and store at 4 °C up to a week.

mTESR1 (STEMCELL TECHNOLOGIES® 05850).

Sterile-filtered water (Sigma-Aldrich® W3500).

Recombinant human BMP 4 (R&D Systems® 314-BP-050).

Blebbistatin (Sigma-Aldrich® B0560).

Stempro34 (GIBCO® 10639-011).

Ascorbic acid (Sigma-Aldrich® A5960).

GlutaMAX (GIBCO® 35050-061).

Recombinant human Activin A (R&D Systems® 328-AC-050).

IWR-1 (Sigma-Aldrich® I0161).

DMEM, no glucose (GIBCO® 11966-025).

L-Lactic acid (Wako® 129-02666).

Lactic medium: 500 ml DMEM without glucose supplemented with 170 μl of L-lactic acid (final concentrate for 4 mM lactic acid solution).

Phosphate-buffered saline without calcium and magnesium (PBS) (WAKO® 045-29795).

2.5 % trypsin (GIBCO® 15090).

1 % collagenase type IV solution: dissolve 10 mg of collagenase IV in 10 ml of PBS, and through with a 0.22 μm pore filter. Aliquot and store at 4 °C up to a week.

Ads buffer: 116 mM NaCl, 20 mM HEPES, 12.5 mM NaH_2PO_4, 5.6 mM glucose, 5.4 mM KCl, and 0.8 mM $MgSO_4$; pH 7.35.

Dissociation buffer: Add 100 μl of 1 % collagenase type IV solution to 100 μl of 2.5 % Trypsin, then fill up to 1 ml by Ads buffer.

4 % paraformaldehyde (PFA) (MUTO PURE CHEMICALS® 33111).

Triton-X (Sigma-Aldrich® T9284).

0.1 % Triton-X: 10 μl of Triton-X in 10 ml of PBS.

Trizma® base (Sigma-Aldrich® T6066).

Tween® 20 (Sigma-Aldrich® P1379).

10× TBS: Dissolve 24.2 g of Trizma® base and 80 g of NaCl in 1,000 ml deionized water, pH 7.6.

1× TBST (1× TBS/0.1 % Tween® 20): Add 100 ml of 10× TBS to 1 ml of TWEEN® 20, then fill up to 1.,000 ml by deionized water.

ImmunoBlock (DS Pharma Biomedical® CTKN001).

Fibronectin (1 mg/ml) (Sigma-Aldrich® F1141).

Fibronectin coating solution (50 μg/ml): Dilute 1 mg/ml of fibronectin by PBS.

DAPI (Molecular Probes® D21490): To make a 5 mg/mL DAPI stock solution: Dissolve the contents of 10 mg in 2 mL of deionized water. For long-term storage, the stock solution can be aliquoted and stored at ≤ -20 °C. For short-term storage, the solution can be kept at 2–6 °C, protected from light. Dilute the DAPI stock solution to 300 nM in PBS.

E4031 (M5060; Sigma-Aldrich).

Chromanol 293B (C2615; Sigma-Aldrich).

Barium chloride (Fluka 34252; Sigma-Aldrich).

Isoproterenol hydrochloride (I6504; Sigma-Aldrich).

Propranolol hydrochloride (P0884; Sigma-Aldrich).

Amphotericin B (Nacalai Tesque 02743-04).

Fluo-4AM (Invitrogen).

Caffeine (SIGMA-ALDRICH).

2.3 Primary Antibodies

Anti-a-Actinin (Sigma-Aldrich® A7811).

Anti-ANP (Santa Cruz® sc-20158).

Anti-MHC (Developmental Studies Hybridoma Bank® MF20).

Anti-TNNT (Thermo Scientific®, NeoMarkers®, 13-11).

Anti-GATA4 (Santa Cruz® sc-1237).

Anti-NKX2.5 (Santa Cruz® sc-8697).

2.4 Secondary Antibodies

Alexa Fluor 488 goat anti-mouse IgG.
Alexa Fluor 594 goat anti-rabbit IgG (all Life Technologies®).

3 Methods

3.1 Cardiac Differentiation of Human iPSCs

With respect to the disease modeling using iPSC-derived cardiomyocytes, to identify the cardiac differentiation protocol with highly reproducibility in many independent iPSC lines is a crucial issue. Thus far, several methods for cardiomyogenesis from iPSCs have been reported, though some were not universal in many independent iPSC lines (8). According to the summary of previous reports, the fact that BMP/Activin and Wnt signaling have a pivotal role for myocardial differentiation is widely accepted and most of current methods are the modification of these signaling manipulation. Herein we introduce one of the representative methods for cardiac differentiation from iPSCs using the stimulation of BMP/Activin signaling in early phase and the inhibition of Wnt signaling in later phase (9).

1. hiPSCs are split at 1:10 ratios, using collagenase type IV (1 mg/dl) as above and grown for 7 days, at which time they reached ~85 % confluence.
2. More than 100 μm-sized splitting iPSC clusters are gathered by 100 μm cell strainer and transfer to 100 mm ultralow attachment culture dish with 10 ml of mTESR1 supplemented with 10 ng/ml of BMP4 and 5 μM of Blebbistatin (day 0).
3. After 24 h incubation, embryoid body (EB) formation should be confirmed and change the medium to Stempro 34 supplemented with 50 μg/ml of ascorbic acid, 2 mM of GlutaMAX, 10 ng/ml of BMP4, and 25 ng/ml of Activin A and incubate the dish for 48 h (day 1–2).
4. Change the fresh Stempro 34 supplemented with 50 μg/ml of ascorbic acid and 2 mM of GlutaMAX. Remove BMP4 and Activin A at this time. Incubate the dish for 36 h (day 4–4.5).
5. Change the fresh Stempro 34 supplemented with 50 μg/ml of ascorbic acid and 2 mM of GlutaMAX and add 2.5 μM of IWR-1; then incubate the dish for 96 h (day 4.5–8.5).
6. Change the fresh Stempro 34 supplemented with 50 μg/ml of ascorbic acid and 2 mM of GlutaMAX. Remove IWR-1 at this time (day 8.5 ~).
7. Change the fresh medium every other day and beating EBs should become visible 2–3 weeks after the induction of differentiated culture condition (*see* **Note 1**).

3.2 In Vitro Purification of iPSC-Derived Cardiomyocytes

iPSC-derived differentiation cells contain wide variety of cells including endodermal cells, mesodermal cells including cardiomyocytes, and ectodermal cells. To investigate accurately the characteristics of iPSC-derived cardiomyocytes, it should be adequate to obtain highly purified cardiomyocytes. Herein we introduce the sophisticated method for in vitro purification of iPSC-derived cardiomyocytes utilizing the cardiomyocyte-specific metabolism (10). In spite of very simple procedure, we can obtain extremely high purified cardiomyocytes.

1. Prepare 18–25 days post-induction in EBs which contain more than 20 % in the incidence of spontaneous beating.
2. Transfer to 50 ml conical tube through 40 μm cell strainer, and wash EBs stayed on cell strainer twice with PBS.
3. Wash 100 mm culture dish twice with PBS and completely remove residual culture medium.
4. Retransfer EBs to 100 mm culture dish in 10 ml lactic medium.
5. 2 days post first change of lactic medium, break up the cells by pipetting up and down several times, and then transfer to 50 ml conical tube through 40 μm cell strainer to remove the medium containing dead cells.
6. Retransfer EBs to 100 mm culture dish in fresh 10 ml lactic medium.
7. 3 days post second change of lactic medium, exchange to fresh 10 ml lactic medium by the same procedure 5 and 6.
8. 5 days post third change of lactic medium, add 5 ml of cardiac differentiated medium.
9. 2 days post addition of cardiac differentiated medium, break up the cells by pipetting up and down several times, then transfer to 50 ml conical tube through 40 μm cell strainer to remove the medium containing dead cells.
10. Retransfer EBs (purified myocardial clusters) to 100 mm culture dish in fresh cardiac differentiated medium.

3.3 Single-Cell Enzymatic Dissociation of iPSC-Derived Cardiomyocytes

1. Collect the cell suspension into a 15 ml conical tube.
2. Centrifuge at 160 × *g* for 5 min, and then discard supernatant.
3. Resuspend a pellet of purified myocardial clusters with 1 ml of dissociation buffer, and transfer to a 1.5 ml tube.
4. Dissociate using magnetic stirring for 30 min in a 37 °C, 5 % CO_2 incubator.
5. Centrifuge the cells, and then discard supernatant.
6. Add 1 ml of differentiated medium, and break up the cells by pipetting up and down several times.
7. Transfer to an adequate-sized dish by each assays.

3.4 Immunofluorescence Staining

1. Dissociated hiPSC-derived cardiomyocytes were plated onto fibronectin-coated Lab-Tek® II 4-chamber glass slides and were allowed to grow for 3 days in differentiated medium.
2. Cells were fixed with 4 % PFA for 30 min at room temperature, permeabilized with 0.1 % Triton-X for 5 min at room temperature, blocked in ImmunoBlock for 30 min at room temperature, and stained using the following primary antibodies and reagents which are 1:200 anti-a-Actinin, 1:100 anti-ANP, 1:100 anti-MHC, 1:100 anti-TNNT, 1:100 anti-GATA4, 1:100 anti-NKX2.5 overnight at 4 °C in ImmunoBlock.
3. Cells were washed four times, for 5 min, with 1× TBST, and then incubated for 1 h at room temperature in the dark with secondary antibodies 1:1,000 Alexa Fluor 488 goat anti-mouse IgG or 1:1,000 Alexa Fluor 594 goat anti-rabbit IgG (Life Technologies) in ImmunoBlock.
4. Cells were washed again as above, nuclei were stained with DAPI, and micro cover glasses were attached to Lab-Tek® II 4-chamber glass slides without the outer frame and imaged with an LSM510 Meta Confocal Microscope.

3.5 The Identification for Electrophysiological Activity of Patient-Specific iPSC-Derived Cells

One of the great benefits for the utilization of patient-specific iPSC-derived cells is to examine directly and repetitively the cellular function of patient-specific alive cells. Here we introduce four methods for the evaluation for electrophysiological activity of iPSC-derived cardiomyocytes (*see* **Notes 2** and **3**).

3.5.1 Field Potential Recordings Using the On-Chip Multi-electrode Array System

The on-chip multi-electrode array system is convenient for analyzing the electrophysiological activity of iPSC-derived cardiomyocytes. We characterize the electrical properties of iPSC-derived cardiomyocytes through the record of field potential which is regarded as similar to body surface electrocardiogram in clinical practice. Since the record can be obtained from cell clusters, it would reflect the electrical status nearby myocardial tissue level, whereas the patch clamp is recorded by a single cell. Furthermore, we can simply evaluate the drug response of multiple myocardial clusters at once, and this method could be a platform for high-throughput drug screening.

1. Multi-electrode array (MEA) chips from Multi Channel Systems (Germany) are coated with 0.001 % fibronectin solution and incubated at 37 °C overnight.
2. Remove the residual fibronectin solution and purified myocardial clusters are plated with culture medium and incubated at 37 °C for several days.
3. Transfer the medium to serum-free once a day before recording.

4. MEA measurements are performed at 37 °C. Obtain the data for approximately 5 min per experiment and subsequently analyze it with MC_Rack (Multi Channel Systems).
5. Record multiple parameters such as beating frequency, the amplitude of each wave, and field potential duration (FPD) defined as the time interval between the initial deflection of the field potential and the maximum local T wave. FPD measurements are usually normalized (corrected FPD: cFPD) to the activation rate using Bazett's correction formulae: cFPD = FPD/(RR interval)$^{1/2}$, where RR indicates the time interval (in seconds) between two consecutive beats (7).
6. Several drugs such as E4031, chromanol 293B, barium chloride, isoproterenol hydrochloride, and propranolol hydrochloride are prepared as 1 or 10 mM stock solutions.
7. After the baseline of field potentials are recorded for 5 min, add the drug to the medium. After 5–10 min of incubation, measure the field potentials for 5–10 min.
8. Perform MEA recordings by investigators blinded to the genotype of the cells.

3.5.2 Patch Clamp Analysis

Whole-cell patch clamp recordings of iPSC-derived cardiomyocytes can be measured using almost the same methods and materials for cardiomyocytes isolated from animals. However, the size and the channel currents of cardiomyocytes derived from iPS cells are usually smaller than those of animal cardiomyocytes. Therefore, it may be difficult to measure currents of some types of channel.

3.5.3 IK+ Measurement

1. Prepare glass bottom dish coated with coating solution (0.1 % gelatin and 2 % fibronectin diluted by PBS). Coating needs at least 15 min.
2. Dissociate iPSC-derived cardiomyocytes to single cells (*see* Section 3.3). Place dissociated cardiomyocytes onto coated glass bottom dish and incubate 37 °C for 60–120 min.
3. Remove the culture medium. Fill normal Tyrode's solution (NaCl 135 mM, KCl 5.4 mM, NaH_2PO_4 0.33 mM, $CaCl_2$ 1.8 mM, $MgCl_2$ 0.5 mM, HEPES 5.0 mM, and glucose 5.5 mM, pH 7.4 adjusted with NaOH) into the iPSC-derived cardiomyocytes attached dish. Set the dish on the stage of microscope of patch clamp system. Axopatch 200B, Digidata 1440A, and pClamp 10.2 (Molecular Devices, USA) can be used for data amplification, acquisition, and analysis, respectively.
4. The resistance of glass pipette is 3–5 MΩ (M ohm) after filling with the internal pipette solution (KOH 60 mM, KCl 80 mM, aspartate 40 mM, HEPES 5 mM, EGTA 10 mM, Mg ATP

5 mM, sodium creatinine phosphate 5 mM, and $CaCl_2$ 0.65 mm, pH 7.2 adjusted with KOH). After sealing and rupture of iPSC-derived cardiomyocytes, perfuse external solution for IK+ recording (*N*-methyl-D-glucamine 149 mM, $MgCl_2$ 5 mM, HEPES 5 mM, nisoldipine 0.003 mM, pH 7.4).

5. Record the currents using voltage clamp protocol. Peak current is recorded with 3 s depolarizing steps from a holding potential of −60 mV to potentials ranging from −60 to +60 mV in 10 mV increments. Tail current is recorded with a 2 s repolarization phase to −40 mV following the step pulse. Pulse frequency was 0.1 Hz.
6. For slow rectifier K+ current (IKs) recording, subtract the current recorded after applying chromanol 293B (10 mM) from IK+. Subtract the current recorded after administrating E4031 (10 mM) from IK+ for rapid rectifier K+ current (IKr) recording.
7. Internal and external solutions for INa or ICa-L recording are given below.

Internal pipette solution for INa+ (mM); CsCl2 130, MgCl2 2, ATP-2Na 5, HEPES 10, EGTA 10, TEA-Cl 20 (pH 7.3 adjusted with CsOH).

External solution for INa+ recording (mM); NaCl 135, CsCl 5.4, $MgCl_2$ 0.53, $CaCl_2$ 2, HEPES-NaOH 5, glucose 5.5, $CdCl_2$ 0.1 (pH 7.4 adjusted with NaOH).

Internal pipette solution for ICa2+ -L (mM); CsOH 60, CsCl 80, aspartate 40, HEPES 5, Mg-ATP 5, phosphocreatine 5, EGTA 10, $CaCl_2$ 0.65 (pH 7.4 adjusted with CsOH).

External solution for ICa^{2+}-L recording (mM); choline chloride 140, CsCl 5, $MgCl_2$ 1, $CaCl_2$ 1.8, glucose 10, HEPES 10 (pH 7.4 adjusted with CsOH).

3.5.4 Ca^{2+} Imaging Assay

Ca^{2+} imaging for iPSC-derived cardiomyocytes has been performed by the same manner as the conventional measurement for other animal myocardial cells. Since the cellular size of human iPSC-derived cardiomyocytes is significantly smaller than the myocardium of other species, the laser exposing time should be reduced by the minimum requirement and the laser intensity should be also adjusted to the proper grade.

1. Dissociated iPSC-derived cardiomyocytes are plated onto 1 % fibronectin-coated 35 mm glass-bottomed dishes (IWAKI) and grow for 2 days with the differentiated medium.
2. Incubate with 5 μM Fluo-4AM (Invitrogen) in Tyrode's solution at 37 °C and wait for loading into cytosol for 30 min.

3. Set up a confocal microscope (LSM 510 Duo, Carl Zeiss) with a ×40 lens (NA = 0.75) for Ca^{2+} imaging.
4. Line scan analysis is acquired at a sampling rate of 2 ms per each line (obtain 10,000 times recordings in 20 s).
5. For the estimation of Ca^{2+} storage in sarcoplasmic reticulum, measure the amplitude of Ca^{2+} transients exposed by the rapid administration of 10 mM caffeine.

4 Notes

1. Distinct iPSC lines show different cardiac differentiation efficiency. It is difficult to compare the cardiac differentiation efficiency among different iPSC lines. Therefore, it is required to generate isogenic iPSCs to show if disease-specific iPSCs would show the difference of cardiac differentiation efficiency.
2. The maturity of iPSC-derived cardiomyocytes affects the result of electrophysiological examination and molecular analysis. To adapt the maturity among the subjects, culture condition should be unified such as differentiation method and differentiation period.
3. Temperature is an important factor to conduct electrophysiological examination. To obtain the data accurately, every equipment and solution should be kept at adequate temperature.

Acknowledgment

This study was supported in part by research grants from the Ministry of Education, Culture, Sports, Science and Technology; Health and Labour Sciences Research Grant; the New Energy and Industrial Technology Development Organization, Japan; the Program for Promotion of Fundamental Studies in Health Science of the National Institute of Biomedical Innovation; Japan Science and Technology Agency; Research Center Network for Realization of Regenerative Medicine "The Program for Intractable Diseases Research utilizing Disease-specific iPS cells," the Nakatomi Foundation; Japan Heart Foundation/Novartis Grant for Research Award on Molecular and Cellular Cardiology SENSHIN Medical Research Foundation; Kimura Memorial Heart Foundation Research Grant; Japan Intractable Diseases Research Foundation, Japan; the Cell Science Research Foundation; the Tokyo Biochemical Research Foundation; Suzuken Memorial Foundation; and the Japan Foundation for Applied Enzymology.

References

1. Takahashi K, Yamanaka S (2006) Induction of pluripotent stem cells from mouse embryonic and adult fibroblast cultures by defined factors. Cell 126(4):663–676. doi:10.1016/j.cell.2006.07.024
2. Takahashi K, Tanabe K, Ohnuki M, Narita M, Ichisaka T, Tomoda K, Yamanaka S (2007) Induction of pluripotent stem cells from adult human fibroblasts by defined factors. Cell 131 (5):861–872. doi:10.1016/j.cell.2007.11.019
3. Egashira T, Yuasa S, Fukuda K (2013) Novel insights into disease modeling using induced pluripotent stem cells. Biol Pharm Bull 36 (2):182–188
4. Lee G, Ramirez CN, Kim H, Zeltner N, Liu B, Radu C, Bhinder B, Kim YJ, Choi IY, Mukherjee-Clavin B, Djaballah H, Studer L (2012) Large-scale screening using familial dysautonomia induced pluripotent stem cells identifies compounds that rescue IKBKAP expression. Nat Biotechnol 30 (12):1244–1248. doi:10.1038/nbt.2435
5. Choi SM, Kim Y, Shim JS, Park JT, Wang RH, Leach SD, Liu JO, Deng C, Ye Z, Jang YY (2013) Efficient drug screening and gene correction for treating liver disease using patient-specific stem cells. Hepatology 57 (6):2458–2468. doi:10.1002/hep.26237
6. Charbord J, Poydenot P, Bonnefond C, Feyeux M, Casagrande F, Brinon B, Francelle L, Auregan G, Guillermier M, Cailleret M, Viegas P, Nicoleau C, Martinat C, Brouillet E, Cattaneo E, Peschanski M, Lechuga M, Perrier AL (2013) High throughput screening for inhibitors of REST in neural derivatives of human embryonic stem cells reveals a chemical compound that promotes expression of neuronal genes. Stem Cells 31(9):1816–1828. doi:10.1002/stem.1430
7. Egashira T, Yuasa S, Suzuki T, Aizawa Y, Yamakawa H, Matsuhashi T, Ohno Y, Tohyama S, Okata S, Seki T, Kuroda Y, Yae K, Hashimoto H, Tanaka T, Hattori F, Sato T, Miyoshi S, Takatsuki S, Murata M, Kurokawa J, Furukawa T, Makita N, Aiba T, Shimizu W, Horie M, Kamiya K, Kodama I, Ogawa S, Fukuda K (2012) Disease characterization using LQTS-specific induced pluripotent stem cells. Cardiovasc Res 95(4):419–429. doi:10.1093/cvr/cvs206
8. Mummery CL, Zhang J, Ng ES, Elliott DA, Elefanty AG, Kamp TJ (2012) Differentiation of human embryonic stem cells and induced pluripotent stem cells to cardiomyocytes: a methods overview. Circ Res 111(3):344–358. doi:10.1161/circresaha.110.227512
9. Weng Z, Kong CW, Ren L, Karakikes I, Geng L, He J, Chow MZ, Mok CF, Keung W, Chow H, Leung AY, Hajjar RJ, Li RA, Chan CW (2014) A simple, cost-effective but highly efficient system for deriving ventricular cardiomyocytes from human pluripotent stem cells. Stem Cells Dev 23(14):1704–1716. doi:10.1089/scd.2013.0509
10. Tohyama S, Hattori F, Sano M, Hishiki T, Nagahata Y, Matsuura T, Hashimoto H, Suzuki T, Yamashita H, Satoh Y, Egashira T, Seki T, Muraoka N, Yamakawa H, Ohgino Y, Tanaka T, Yoichi M, Yuasa S, Murata M, Suematsu M, Fukuda K (2013) Distinct metabolic flow enables large-scale purification of mouse and human pluripotent stem cell-derived cardiomyocytes. Cell Stem Cell 12(1):127–137. doi:10.1016/j.stem.2012.09.013

Molecular Bases of Disease:

HTRA1 (High Temperature Requirement A Serine Peptidase 1) Gene Is Transcriptionally Regulated by Insertion/Deletion Nucleotides Located at the 3′ End of the *ARMS2* (Age-related Maculopathy Susceptibility 2) Gene in Patients with Age-related Macular Degeneration

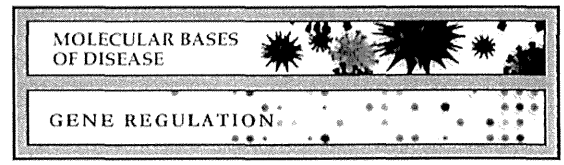

Daisuke Iejima, Takeshi Itabashi, Yuich Kawamura, Toru Noda, Shinsuke Yuasa, Keiichi Fukuda, Chio Oka and Takeshi Iwata

J. Biol. Chem. 2015, 290:2784-2797.
doi: 10.1074/jbc.M114.593384 originally published online December 17, 2014

THE JOURNAL OF BIOLOGICAL CHEMISTRY VOL. 290, NO. 5, pp. 2784–2797, January 30, 2015

HTRA1 (High Temperature Requirement A Serine Peptidase 1) Gene Is Transcriptionally Regulated by Insertion/Deletion Nucleotides Located at the 3′ End of the *ARMS2* (Age-related Maculopathy Susceptibility 2) Gene in Patients with Age-related Macular Degeneration*

Received for publication, July 1, 2014, and in revised form, December 15, 2014 Published, JBC Papers in Press, December 17, 2014, DOI 10.1074/jbc.M114.593384

Daisuke Iejima[‡], Takeshi Itabashi[‡], Yuich Kawamura[‡], Toru Noda[§], Shinsuke Yuasa[¶], Keiichi Fukuda[¶], Chio Oka[‖], and Takeshi Iwata[‡1]

From the [‡]Division of Molecular and Cellular Biology, National Institute of Sensory Organs, and the [§]Division of Ophthalmology, National Hospital Organization Tokyo Medical Center, Tokyo 152-8902, Japan, the [¶]Department of Cardiology, Keio University School of Medicine, Tokyo 160-8582, Japan, and the [‖]Division of Gene Function in Animals, Nara Institute of Science and Technology, Nara 630-0101, Japan

Background: The biological function of insertion/deletion sequences associated with AMD has not been fully characterized.
Results: The *HTRA1* regulatory region contains an insertion/deletion sequence that is significantly up-regulated in retinal neuronal cell lines.
Conclusion: *HTRA1* expression is enhanced by a mutation in the insertion/deletion in the *HTRA1* regulatory region.
Significance: This is the characterization of the *HTRA1* regulatory elements and the effect of insertion/deletion sequences associated with AMD.

Dry age-related macular degeneration (AMD) accounts for over 85% of AMD cases in the United States, whereas Japanese AMD patients predominantly progress to wet AMD or polypoidal choroidal vasculopathy. Recent genome-wide association studies have revealed a strong association between AMD and an insertion/deletion sequence between the *ARMS2* (age-related maculopathy susceptibility 2) and *HTRA1* (high temperature requirement A serine peptidase 1) genes. Transcription regulator activity was localized in mouse retinas using heterozygous *HtrA1* knock-out mice in which *HtrA1* exon 1 was replaced with β-galactosidase cDNA, thereby resulting in dominant expression of the photoreceptors. The insertion/deletion sequence significantly induced *HTRA1* transcription regulator activity in photoreceptor cell lines but not in retinal pigmented epithelium or other cell types. A deletion construct of the *HTRA1* regulatory region indicated that potential transcriptional suppressors and activators surround the insertion/deletion sequence. Ten double-stranded DNA probes for this region were designed, three of which interacted with nuclear extracts from 661W cells in EMSA. Liquid chromatography-mass spectrometry (LC-MS/MS) of these EMSA bands subsequently identified a protein that bound the insertion/deletion sequence, LYRIC (lysine-rich CEACAM1 co-isolated) protein. In addition, induced pluripotent stem cells from wet AMD patients carrying the insertion/deletion sequence showed significant up-regulation of the *HTRA1* transcript compared with controls. These data suggest that the insertion/deletion sequence alters the suppressor and activator *cis*-elements of *HTRA1* and triggers sustained up-regulation of *HTRA1*. These results are consistent with a transgenic mouse model that ubiquitously overexpresses *HtrA1* and exhibits characteristics similar to those of wet AMD patients.

Recent genome-wide association studies have identified more than 19 susceptibility genes associated with age-related macular degeneration (AMD)[2] (1). Among these genes, two loci have been highly associated with AMD, and these include the *CFH* (complement factor H) gene on chromosome 1q32 and the *ARMS2/HTRA1* (age-related macular degeneration susceptibility 2/high temperature requirement A1) gene on chromosome 10q26. Although a strong association of *CFH* Y402H (rs1061170) with Caucasians with dry AMD has been established (2, 3), this locus has not been associated with the majority of Japanese patients with wet AMD (4). Rather, *ARMS2/HTRA1* is the region most strongly associated with wet AMD in Japanese patients (5, 6). Moreover, the single nucleotide polymorphism (SNP), rs10490924, was shown in a single linkage disequilibrium (LD) block to increase the risk of wet AMD in both Caucasian and Japanese AMD populations (6). This LD block included the entire *ARMS2* gene and a portion of *HTRA1* exon 1 (Fig. 1). However, genome-wide association studies alone are insufficient to distinguish between these two candidate genes. Previous reports have identified an insertion/deletion region ~443 bp in length that immediately follows the

* This work was supported by Japanese Ministry of Health, Labor, and Welfare Grant 10103254 and National Hospital Organization of Japan Grant 09005752 (to T. I.). This work was also supported by Japan Society for the Promotion of Science Grant 23890258 (to D. I.).
[1] To whom correspondence should be addressed. Tel./Fax: 81-3-34111026; E-mail: takeshi_iwata@kankakuki.go.jp.

[2] The abbreviations used are: AMD, age-related macular degeneration; LD, linkage disequilibrium; RPE, retinal pigment epithelium; PCV, polypoidal choroidal vasculopathy; iPSC, induced pluripotent stem cell; TLR, Toll-like receptor.

second exon of *ARMS2* within the regulatory element of *HTRA1* (7, 8). This finding led to confusion as to whether a single gene or both *ARMS2* and *HTRA1* are involved in AMD. *ARMS2* is a recent gene evolutionarily and is within the primate lineage (7, 9). Its protein product, ARMS2, has been shown to localize to the mitochondria of the inner segment of the photoreceptor (7) and to interact with fibulin-6 in the extracellular matrix of the choroid (10). However, details regarding the biological function(s) of ARMS2 remain unclear (7, 9, 10). In contrast, *HTRA1* has been characterized to some extent. HTRA1 belongs to the HTRA serine protease family, which is highly conserved from microorganisms to multicellular organisms, including humans (11). Several cellular and molecular studies have suggested that HTRA1 plays a key role in regulating various cellular processes via the cleavage and/or binding of pivotal factors that participate in cell proliferation, migration, and cell fate (12–15). Recently, up-regulation of human *HTRA1* expression in the mouse retinal pigment epithelium (RPE) was shown to induce a branching network of choroidal vessels and polypoidal lesions and severe degeneration of the elastic lamina and tunica media of the choroidal vessels, similar to that observed in AMD and PCV patients (16, 17). A mutation in *HTRA1* has also been associated with a hereditary form of familial cerebral small vessel disease (CARASIL (cerebral autosomal recessive arteriopathy with subcortical infarcts and leukoencephalopathy)) (18). The original report by Dewan *et al.* (19) described the up-regulation of HTRA1 in fibroblasts obtained from AMD patients. This result was both confirmed and denied by several other groups and was also subjected to a regulatory element characterization assay containing the insertion/deletion sequence (7, 8). However, the results obtained were based on transcription regulator activity that was measured using the human RPE cell line, ARPE19. On the basis of previous study, the purpose of this study is to characterize transcription regulation of *ARMS2 and HTRA1* genes in wet form AMD.

EXPERIMENTAL PROCEDURES

Subjects—A total of 226 Japanese patients with typical wet AMD without PCV (average age, 74.68 ± 8.86 years) were classified as 5b according to Seddon *et al.* (20). In addition, 228 non-AMD Japanese individuals (average age, 75.22 ± 7.23 years) were recruited as controls for this study (Table 1). All patients were diagnosed by fundus observation or by fluorescein/indocyanine green angiographic findings. For the controls, no signs of early AMD, such as soft drusen or alterations of the retinal pigment epithelium in the macula area, were observed ophthalmoscopically. Informed consent was obtained from all of the patients and controls, and the procedures performed conformed to the tenets of the Declaration of Helsinki.

DNA Isolation and Sequencing—Human DNA was extracted from blood samples using a Magtration System 8Lx (Precision System Science Co., Ltd., Tokyo, Japan). The *PLEKHA1-ARMS2-HTRA1* region of genomic DNA was amplified from both control and AMD patient samples using the primers listed in Table 1. PCR amplifications for all primer sets were performed in a 20-μl volume containing 100 ng of genomic DNA and 1 unit of *Taq* polymerase (PrimerStar, Takara Bio Co. Ltd., Japan) for 35–40 cycles of amplification. Amplified PCR products were then purified using an ExoSAP-IT kit (GE Healthcare) and were sequenced using a BigDye Terminator version 3.1 sequencing kit (Invitrogen) and an ABI 3130 Genetic Analyzer.

TABLE 1
Primers used for sequencing

Primer name	Sequence
PLEKHA1-ARMS2-F1	CCCCATGCTTTCAGGGTTCACC
PLEKHA1-ARMS2-R1	GGGGTCTCATTCTGTTGTCCAGGC
PLEKHA1-ARMS2-F2	TGTTCCCAGCCTCTCCCCACTCTT
PLEKHA1-ARMS2-R2	GAACCACTTCTCCCAGCCAAACACT
PLEKHA1-ARMS2-F3	GTTCAGTGGCGCAATCTCGGC
PLEKHA1-ARMS2-R3	CCTCATGCACTGCTAGTGGGATTGT
PLEKHA1-ARMS2-F4	CAGGCTGGAGTGCAATGGTGTGAT
PLEKHA1-ARMS2-R4	GGAGGATTGCTTGAGCCCAGGAC
PLEKHA1-ARMS2-F5	CTACGTGGCGGGCGCTGTCT
PLEKHA1-ARMS2-R5	CTGTGTTGGCTGGACTCGGTAGCT
ARMS2-F1	CTGAGCCGAGGAGTATGAGG
ARMS2-R1	CAGGAACCACCGAGGAGGACAGAC
ARMS2-F2	TCCCTGAGACCACCCAACAA
ARMS2-R2	CGCGCTCACATTTAGAACAT
ARMS2-F3	GCGCTTTGTGCTTGCCATAGT
ARMS2-R3	CCAAAATAGGACAAAGGTGAGG
ARMS2-F4	GTGAAACCCCATCTCTACTAAAAATACAG
ARMS2-R4	CCCACATCAGTTCAGTTAGGTTCGGTTCAG
ARMS2-F5	GCTTGGCAGTCACATGTAGTTAGT
ARMS2-R5	CAGGCCTTGGCACGGTATTCT
ARMS2-HTRA1-F2	CAAGGCCTGGTGAGTGAGAAATGAGTT
ARMS2-HTRA1-R2	GAGGGGGTGGAGAATGGGTAAGAGG
ARMS2-HTRA1-F3	TCCACTTCGGCCGACACTTCCTC
ARMS2-HTRA1-R3	TGCCTTTCTTTGCCCACATCTCC
ARMS2-HTRA1-F4	TGGGGGCACGAGGATGGAAGAG
ARMS2-HTRA1-R4	AGGGAATGAGCGGACCGAAAACAGT
ARMS2-HTRA1-F5	TGGGCAAAGAAAGGCACAGAGACC
ARMS2-HTRA1-R5	TGGGGCAGATGGAATTAAAAGGACA
ARMS2-HTRA1-F6	CCGCAAAGCAGTGGGGAAGTT
ARMS2-HTRA1-R6	CCTCATCCCGAACCCTCAAACCTC
ARMS2-HTRA1-F7	TTGAGGGGGCTTATAGGTATTTGGAGTT
ARMS2-HTRA1-R7	GGGTGGCATGCGTGTCCGTATTC
ARMS2-HTRA1-F8	CCCAACGGATGCACCAAAGATTC
ARMS2-HTRA1-R8	CCCGGTCACGCGCTGGTTCT
ARMS2-HTRA1-F9	ACGCATGCCACCCACAACAACTTTT
ARMS2-HTRA1-R9	GCGGGATCTGCATGGCGACTCT

Cell Culture—The mouse photoreceptor cell line, 661W, and the rat retinal ganglion cell line, RGC5, were cultured in Dulbecco's modified Eagle's medium (DMEM) containing 10% fetal bovine serum (FBS) at 37 °C in 5% CO_2. The human RPE cell line, ARPE19, was cultured in DMEM/F-12 containing 15% FBS at 37 °C in 5% CO_2.

Transcription Regulator Activity Assay—The *ARMS2* regulatory region and the *HTRA1* regulatory region were amplified and cloned into the pGL4.10 (Luc2) luciferase vector (Promega, WI) (Table 2). Insertion/deletion variants were also constructed using a KOD mutagenesis kit (Toyobo, Osaka, Japan). For the luciferase assays performed, 661W cells, RGC5 cells, and ARPE19 cells were seeded in 96-well plates (1×10^4 cells/well) 24 h before transfection. Transfections were performed using Lipofectamine LTX with Plus reagent (Invitrogen). A firefly luciferase gene was integrated into a reporter vector to normalize the activity of both transcription regulators. Luciferase activity was detected using the Dual-Glo luciferase assay system (Promega) and a microplate reader (Plate Chameleon, Hidex, Turku, Finland).

Preparation of Induced Pluripotent Stem Cells (iPSCs) from Controls and AMD Patients—Human iPSCs were established by infecting circulating T cells obtained from the peripheral blood of human AMD patients with the Sendai virus as described previously (21, 22). Briefly, peripheral blood mononuclear cells were obtained from donors by the centrifugation

TABLE 2
Primer used for cloning

Number	Oligonucleotide sequence[a]	Forward/Reverse	Enzyme site	Description	Type
1	ACGT**CTCGAG**GCCTCGCAGCGGTGACGAG	Reverse	XhoI	Reverse primer	Normal, in/del
2	ACGT**GAGCTC**AGATGCAGCCCAATCTTCTCCTAACA	Forward	SacI	Normal or in/del: full-length	Normal, in/del
3	ACGT**GAGCTC**CCCCTCCTTTCTCTCCCGGGTG	Forward	SacI	Normal or in/del: Δ82	Normal, in/del
4	ACGT**GAGCTC**TGTCTAGCAGTGTCTACCCTGTGGCA	Forward	SacI	Normal: Δ298	Normal
5	ACGT**GAGCTC**GGTGTACCTGCTGTTAAAGGAGGT	Forward	SacI	Normal: Δ384	Normal
6	ACGT**GAGCTC**AATGGGTGAGTAGGGATGGATTACA	Forward	SacI	Normal: Δ543	Normal
7	ACGT**GAGCTC**AATGGGTGAGTAGGGATGGATTA	Forward	SacI	In/del: Δ148	In/del
8	AATGGGTGAGTAGGGATGGATTACACC	Inverse-F		In/del: Δin/del-F	In/del
9	CCGGGAGAGAAAGGAGGGCAA	Inverse-R		In/del: Δin/del-R	In/del

[a] Boldface sequence, restriction enzyme site for cloning.

TABLE 3
EMSA probe sequence

Number	Type	Probe sequence
1	Sense	AGATGCAGCCCAATCTTCTCCTAACATCTGGATTCCTCTC
	Antisense	GAGAGGAATCCAGATGTTAGGAGAAGATTGGGCTGCATCT
2	Sense	GATTCCTCTCTGTCACTGCATTCCCTCCTGTCATCCTGCC
	Antisense	GGCAGGATGACAGGAGGGAATGCAGTGACAGAGAGGAATC
3	Sense	TCATCCTGCCTTTGTTTTCTTGCCCTCCTTTCTCTCCCGG
	Antisense	CCGGGAGAGAAAGGAGGGCAAGAAAACAAAGGCAGGATGA
4	Sense	GGTGTACCTGCTGTTAAAGGAGGTTACGACCTCTGATGCT
	Antisense	AGCATCAGAGGTCGTAACCTCCTTTAACAGCAGGTACACC
5	Sense	ATGCTGGGGTGGCCAGAGGGGATGGGAGTGGGTCTGGCAC
	Antisense	GTGCCAGACCCACTCCCATCCCCTCTGGCCACCCCAGCAT
6	Sense	GGCACTCTGAGGAAAGGGGGTGAAACCAGCTGAGAAGTCA
	Antisense	TGACTTCTCAGCTGGTTTCACCCCCTTTCCTCAGAGTGCC
7	Sense	AGTCATCTTTTACCTGCTGGCATGGCCCCAGCCAGGGTTC
	Antisense	GAACCCTGGCTGGGGCCATGCCAGCAGGTAAAAGATGACT
8	Sense	CCCCAGCCAGGGTTCTGTTGCTATGGGAGAATGGGTGAGT
	Antisense	ACTCACCCATTCTCCCATAGCAACAGAACCCTGGCTGGGG
9	Sense	TCTCTCCCGGTTATTAATTAATTAACTAAAATTAAATTAT
	Antisense	ATAATTTAATTTTAGTTAATTAATTAATAACCGGGAGAGA
10	Sense	AATTATTTAGTTAATTTAATTAACTAAACTAATGGGTGAG
	Antisense	CTCACCCATTAGTTTAGTTAATTAAATTAACTAAATAATT

of heparinized blood over a Ficoll-Paque PREMIUM (GE Healthcare) gradient, according to the manufacturer's instructions. The peripheral blood mononuclear cells were then cultured at 37 °C in 5% CO_2 with plate-bound anti-CD3 monoclonal antibodies (BD Pharmingen) in GT-T502 medium (Kohjin Bio, Sakado, Japan) supplemented with recombinant interleukin-2 (IL-2) at 175 Japan reference units/ml. After 5 days, activated peripheral blood mononuclear cells were collected and transferred to 6-well plates (1.5×10^6 cells/well) coated with anti-CD3 monoclonal antibodies, and the cells were incubated for an additional 24 h. A solution containing Sendai virus vectors that individually carried OCT3/4, SOX2, KLF4, and c-MYC (DNAVEC Inc., Japan) was added to each well. At 24 h postinfection, the medium was changed to fresh CT-T502 medium. At 48 h postinfection, the cells were collected and transferred to a 10-cm dish that contained mitomycin C-inactivated mouse embryonic fibroblast feeder cells (6×10^4 to 6×10^5 cells/dish). After an additional 24 h of incubation, the medium was changed to iPSC medium, which consisted of DMEM/F-12 medium (Sigma) supplemented with 20% knockout serum replacement (Invitrogen), 1 mM L-glutamine, 1 mM non-essential amino acids, 0.1 mM β-mercaptoethanol, 50 units of penicillin, 50 mg/ml streptomycin, and 4 ng/ml basic fibroblast growth factor (Wako Pure Chemical Industries, Osaka, Japan). The iPSC medium was changed every other day until colonies were picked. The generated iPSCs were maintained on irradiated mouse embryonic fibroblast feeder cells in iPSC medium. Culture medium for the iPSCs was changed every 2 days, and the cells were passaged using 1 mg/ml collagenase IV every 5–6 days.

EMSA—Nuclear extracts were prepared with a CelLytic nuclear extraction kit (Sigma), according to the manufacturer's protocol. The nuclear protein concentration of each sample was determined using a BCA protein assay kit (Thermo Scientific).

EMSA probes were 40 bp in length and are listed in Table 3. Probes 1–3 were designed to cover non-insertion/deletion and insertion/deletion regions (non-insertion/deletion, bp −4320 to −4220; insertion/deletion, bp −3936 to −3836). Probes 4–8 were designed to cover the non-insertion/deletion regulatory region (non-insertion/deletion, bp −3936 to −3777). Probes 9 and 10 were designed to cover the insertion/deletion region (insertion/deletion, −3836 to −3782 bp). Double-stranded DNA probes were biotin-labeled using a LightShift chemiluminescent EMSA kit (Thermo Scientific) and then were mixed with nuclear extracts. After 20 min, the samples were subjected to electrophoresis on 7% EMSA gels. After electrophoresis, the samples were transferred onto Biodyne B precut modified nylon membranes (Thermo Scientific). The membranes were cross-linked in a UV transilluminator for 15 min and then were incubated with blocking buffer and streptavidin-horseradish peroxidase conjugates. Bound conjugates were detected using a molecular imager (ChemiDoc XRS+, Bio-Rad).

RT-PCR—The iPSCs were removed from the feeder cells and were rinsed twice with PBS. Total cellular RNA was extracted with TRIzol reagent (Invitrogen), according to the manufactur-

er's instructions. RNA concentrations were determined by measuring absorption values at 260 nm/280 nm. Reverse transcription was performed using a SuperScript first strand synthesis system for RT-PCR kit (Invitrogen). Primer sequences for human *OCT3/4*, *NANOG*, *SOX2*, and *GAPDH* as well as the associated PCR detection methods were created and performed according to Seki *et al.* (21). The primers used to detect human *HTRA1* included AACTTTATCGCGGACGTGGTGGAG (forward) and TGATGGCGTCGGTCTGGATGTAGT (reverse).

Quantitative RT-PCR—Total RNA was isolated from human iPSCs with an RNeasy minikit (Qiagen, Hilden, Germany) according to the manufacturer's instructions. An aliquot of each sample was reverse-transcribed using a high capacity cDNA reverse transcription kit (Invitrogen) to obtain single-stranded cDNAs. Using an ABI STEP-One real-time PCR system (Invitrogen) with TaqMan probes for human *HTRA1*, quantitative RT-PCR was performed according to the manufacturer's instructions. All of the reactions were run in triplicate using the ΔCt method, and detection of human *GAPDH* was used as an internal control.

Liquid Chromatography-Mass Spectrometry (LC-MS/MS)—Nuclear extract of 661W cells (50 μg) was combined with 100 pmol of biotin-labeled, double-stranded DNA probes in DNAP buffer (20 mM HEPES, 80 mM KCl, 1 mM MgCl, 0.2 mM EDTA, 10% glycerol, 0.1% Triton X-100, 0.5 mM DTT). This proteins/probes mixture was incubated at 4 °C for 30 min before 50 ml of Dynabeads M280 streptavidin (Invitrogen) was added. The mixture was incubated at 4 °C for 30 min. The beads-probes-protein complex was then washed with 500 μl of DNAP buffer three times for 30 min at 4 °C. The washed complexes were mixed with 30 μl of SDS-PAGE sample buffer (Bio-Rad) and were boiled for 5 min at 100 °C. The boiled samples were quenched on ice for 5 min before being separated by 7.5% SDS-PAGE. Bands of interest were cut out of the gel and were processed for in-gel digestion for further LC-MS/MS analysis. A Thermo LTQ system (Thermo Scientific) and Scaffold 4 data analysis software (Matrix Science) were used.

Immunohistochemistry—Eyes from wild type, *HtrA1* knockout, and *HtrA1* transgenic mice (12, 16, 23) were resected and immersed in a fixative containing 4% paraformaldehyde overnight at 4 °C. The eyes were embedded in OCT compound and frozen on dry ice. Sections of the frozen eyes (10 μm) were washed with 0.1% Tween 20, PBS (PBST) prior to permeabilization with 0.3% Triton X-100, PBS for 15 min. After the sections were washed in 0.1% PBST, they were incubated with blocking solution for 1 h, followed by an overnight incubation at 4 °C with anti-rabbit HtrA1 antibodies (Abcam) in PBS, 2% BSA. The sections were washed in 0.1% PBST three times and then were incubated with Alexa Fluor 488-conjugated anti-rabbit IgG antibodies (1:1000; Invitrogen) and DAPI (Dojindo, Japan) for nuclear staining at room temperature. After 1 h, the sections were mounted with Ultramount aqueous permanent mounting medium (DakoCytomation, Glostrup, Denmark) and were analyzed using a confocal fluorescence laser microscope (LSM 700, Zeiss).

In Situ Hybridization—Eyes from *HtrA1* heterozygous mice were removed and immersed in 5% formaldehyde overnight at 4 °C. The eyes were then embedded in paraffin and sectioned (10 μm). *In situ* hybridization was performed using a QuantiGene™ ViewRNA system (Affymetrix, Santa Clara, CA) using HtrA1 and LacZ probes according to the manufacturer's instructions.

Western Blotting—Total proteins were extracted from mouse brain tissues in ice-cold TNE buffer (10 mM Tris-HCl, 100 mM NaCl, 10 mM EDTA, 0.1% Nonidet P-40) containing protease and phosphatase inhibitors (Roche Applied Science). Protein concentrations of the extracts were determined using a BCA assay kit (Thermo Scientific). Equal amounts of protein (10 μg/lane) were separated by 7.5% SDS-PAGE and were transferred to PVDF membranes (Trans-Blot Turbo, Bio-Rad). The membranes were then incubated with an anti-mouse HtrA1 antibody (1:100; Abcam) and an anti-α-tubulin antibody (1:1000; Abcam). A FluorChem Western blot imaging station (ChemiDoc XRS+, Bio-Rad) and image analysis software (Image Lab, Bio-Rad) were used to calculate and normalize the pixel value of each protein band.

RESULTS

Sequencing of ARMS2-HTRA1 Loci in Controls and AMD Patients—To determine the genomic sequence of the LD block represented by the SNP, rs10490924, in association with AMD (6, 19, 24), ~10.5 kbp of the LD block (NC_000010.10) was sequenced for 228 controls and 226 AMD patients. Two unique sequences were identified in the regulatory region of *ARMS2* and *HTRA1* (Fig. 1). A C-to-A (C/A) variant was identified in the regulatory region of *ARMS2*, −550 bp upstream of exon 1 (Fig. 1, *A* and *B*), and an insertion/deletion variant was identified immediately following the *ARMS2* exon 2 in the regulatory region of *HTRA1*, −3777 bp upstream of exon 1 (Fig. 1, *A* and *C*). Sequence variations in both transcription regulators were in complete LD with SNP rs10490924, thereby suggesting that AMD and PCV pathogenesis are directly associated with these variants.

The Effect of C/A and Insertion/Deletion Variants on ARMS2 and HTRA1 Regulatory Region Activity—To date, two hypotheses have been proposed to account for the increased risk of AMD that is observed. These involve an increase in the transcription of *HTRA1* and/or the presence of unstable *ARMS2* mRNA (7, 19, 24). To investigate the first hypothesis, regulator activity for *ARMS2* was assayed using constructs covering the regulatory region from −1,000 to +1 bp and from −600 to +1 bp. Both of these regions contain the C/A repetitive variant (Fig. 1*D*). Regulatory region activity was not detected for either the non-C/A or C/A variants of differing length for retinal cell lines (ARPE19, 661W, and RGC5 tested) (Fig. 1, *E–G*). Next, regulator activity of *HTRA1* was assayed for the −4,320 to +1 bp region of the non-insertion/deletion regulatory region and for the −3,936 to +1 bp region of the insertion/deletion regulatory region (Fig. 1*H*). Both regions had common sequences on both ends of the regulatory region. Transcription regulator activity was not found to be affected by the insertion/deletion variants in the ARPE19 cell line (Fig. 1*I*). However, activity of the insertion/deletion regulator was significantly up-regulated compared with the activity of the non-insertion/deletion regulator in both the 661W and RGC5 cell lines, by ~2- and 3-fold, respectively (Fig. 1, *J* and *K*). Moreover, *HTRA1* non-insertion/

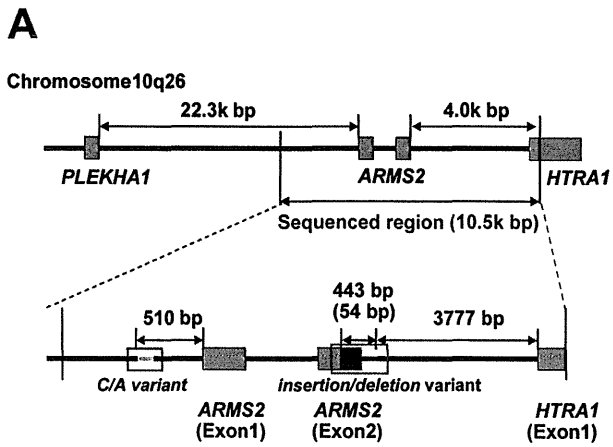

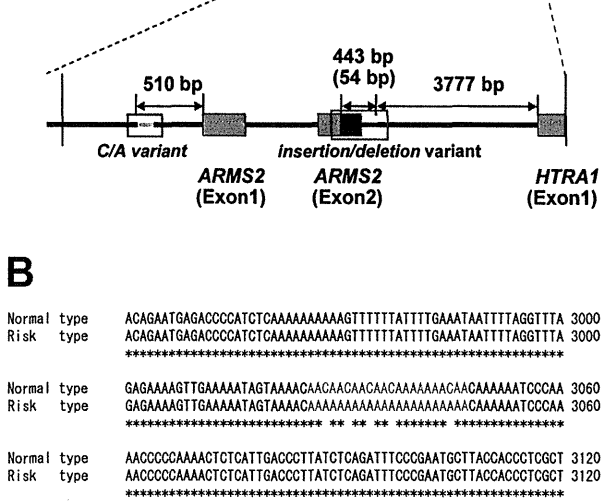

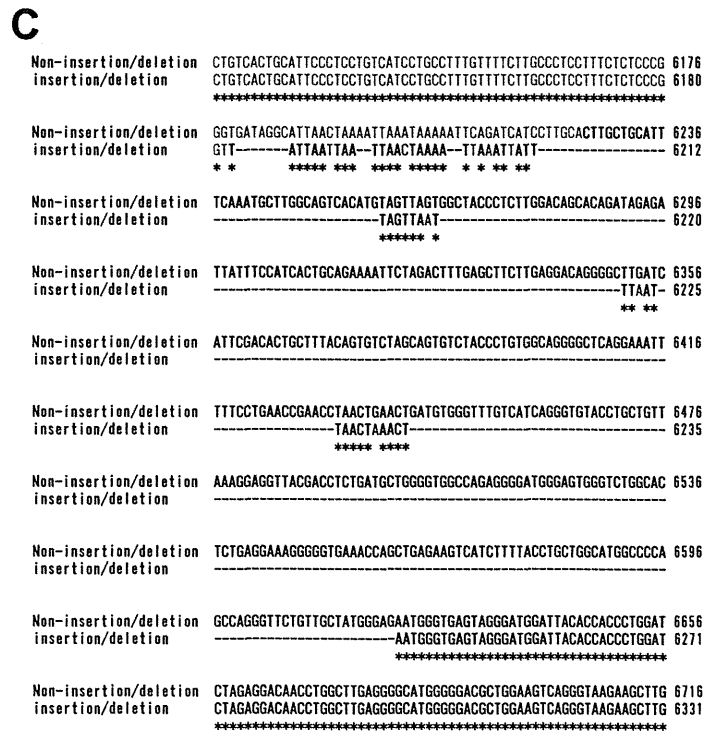

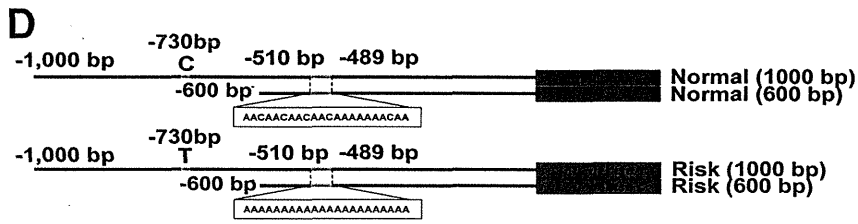

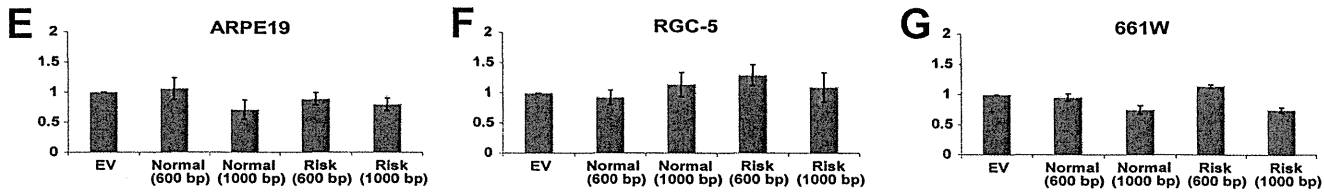

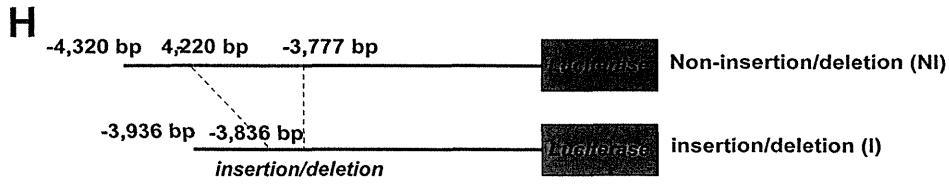

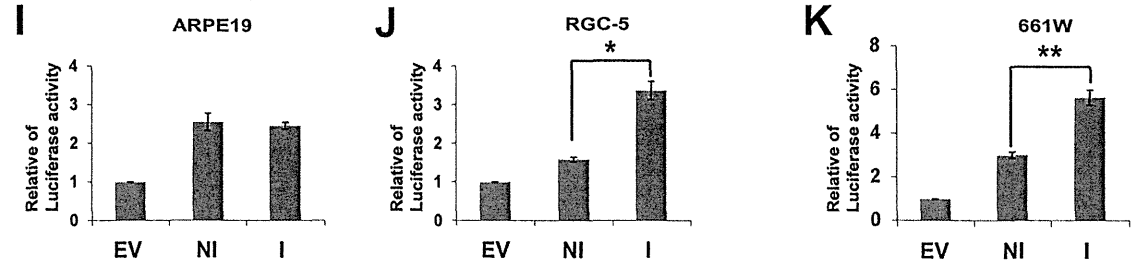

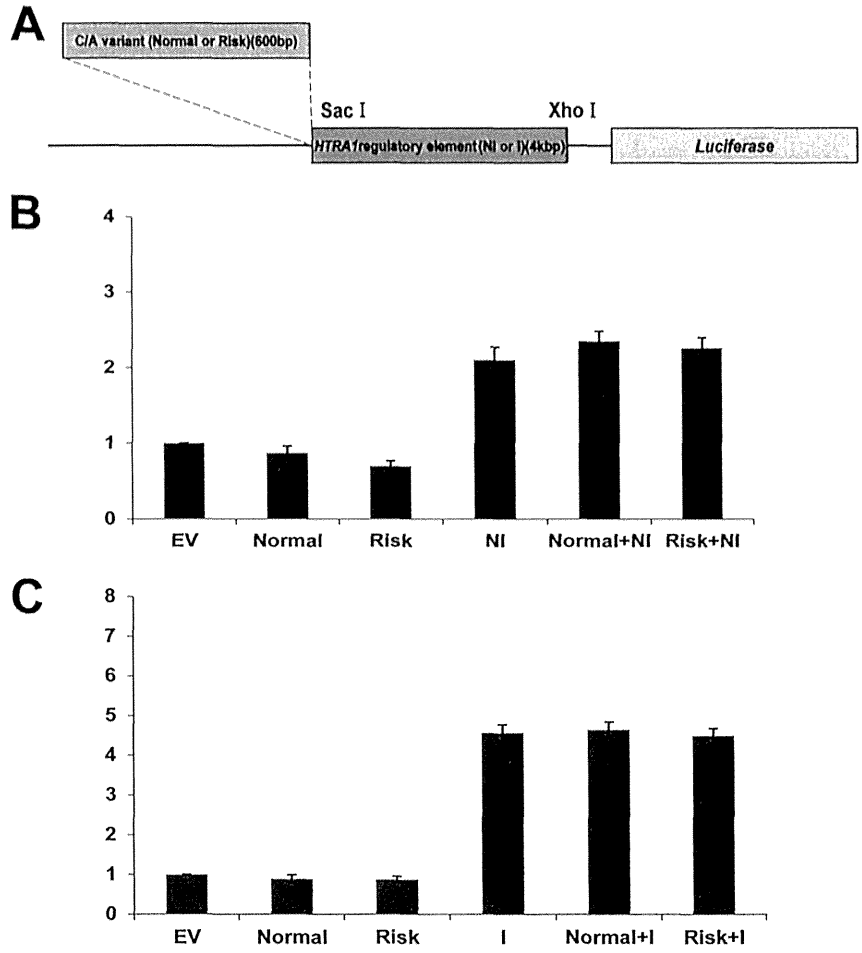

FIGURE 2. **The effect of the *ARMS2* C/A variant on the *HTRA1* transcription regulator.** *A*, schematic diagram of the C/A variant plus *HTRA1* regulatory element in the constructs used for luciferase assays (*blue region*, 600-bp *AMRS2* transcription regulatory region (contains C/A variant); *orange region*, region that contains the *HTRA1* regulatory element; *yellow region*, the luciferase reporter gene). *B*, C/A variant plus non-insertion/deletion type *HTRA1* regulatory element activity in 661W cells. *C*, C/A variant plus insertion/deletion type *HTRA1* regulatory element activity in 661W cells. *Error bars*, S.D. *EV*, empty vector; *Normal*, normal type C/A variant; *Risk*, risk type C/A variant; *NI*, non-insertion/deletion type *HTRA1* regulatory element; *I*, insertion/deletion type *HTRA1* regulatory element.

deletion regulator activity was not detected in the latter, similar to the empty vector. However, when the non-insertion/deletion regulator was replaced with the insertion/deletion regulator in the 661W and RGC5 cell lines, *HTRA1* regulatory element activity increased 2- and 3-fold, respectively (Fig. 1*J*). To test whether C/A variants in the transcription regulatory region of *ARMS2* influence *HTRA1* gene expression, both normal and risk type *ARMS2* C/A variant (Fig. 2*A*) were cloned and fused to the *HTRA1* transcription regulator of the non-insertion/deletion and insertion/deletion constructs. Luciferase levels were subsequently measured following transfection of these vectors (Fig. 2*A*). Neither the normal nor the risk type, C/A variants affected *HTRA1* transcription regulator activity (Fig. 2, *B* and *C*).

Endogenous Transcription Regulator Activity and Protein and mRNA Expression of HtrA1 in Mouse Retina Tissues—To examine the localization of HtrA1 in the retina, eye sections from both wild type and mutant (HtrA1 knock-out, HtrA1 transgenic) mice were stained with an anti-mouse HtrA1 antibody (Fig. 3*A*). In both wild type and HtrA1-Tg mouse sections,

FIGURE 1. **Transcription regulatory region of *ARMS2* and *HTRA1*.** *A*, a schematic diagram of the transcription regulatory region of *ARMS2* and *HTRA1*. Sequencing of the indicated transcription regulatory region spanned 10.5 kbp and was performed for both AMD and non-AMD controls. Two unique sequences, a C/A repeat variant in the *ARMS2* transcription regulator (indicated with a *blue box*) and an insertion/deletion variant downstream of exon 2 of *ARMS2* (indicated with a *red box*), were identified in a patient with AMD that carried the SNP, rs10490924. *B*, characteristic C/A mutations present in the *ARMS2* transcription regulatory region (*blue*, C/A variant; *red*, C to A substitution). *C*, the insertion/deletion mutations present in the *HTRA1* transcription regulatory region (*blue*, ARMS2 exon 2 region; *red*, point mutations). *D–G*, analysis of *ARMS2* transcription regulator activity using a luciferase assay system. *D*, four luciferase vectors were generated to analyze *ARMS2* transcription regulator activity: normal (1,000 bp), normal (600 bp), risk (1,000 bp), and risk (600 bp). The 1,000-bp sequence contained a C/T SNP in the upper 730-bp region from *ARMS2* exon 1. *ARMS2* transcription regulator activity detected in ARPE19 cells (*E*), RGC-5 cells (*F*), and 661W cells (*G*). *Error bars*, S.D. *H–K*, *HTRA1* transcription regulator activity detected in various retinal cell lines. *H*, schematic diagram of the *ARMS2-HTRA1* constructs used in the luciferase assays performed (*black line*, common regulator sequence; *blue line*, non-insertion/deletion regulator unique sequence; *red line*, insertion/deletion regulator unique sequence). Full-length *HTRA1* transcription regulator activity detected in ARPE19 cells (*I*), RGC5 cells (*, $p = 7.5 \times 10^{-6}$) (*J*), and 661W cells (**, $p = 1.07 \times 10^{-6}$) (*K*). *Error bars*, S.D. *EV*, empty vector; *NI*, non-insertion/deletion regulator; *I*, insertion/deletion regulator.

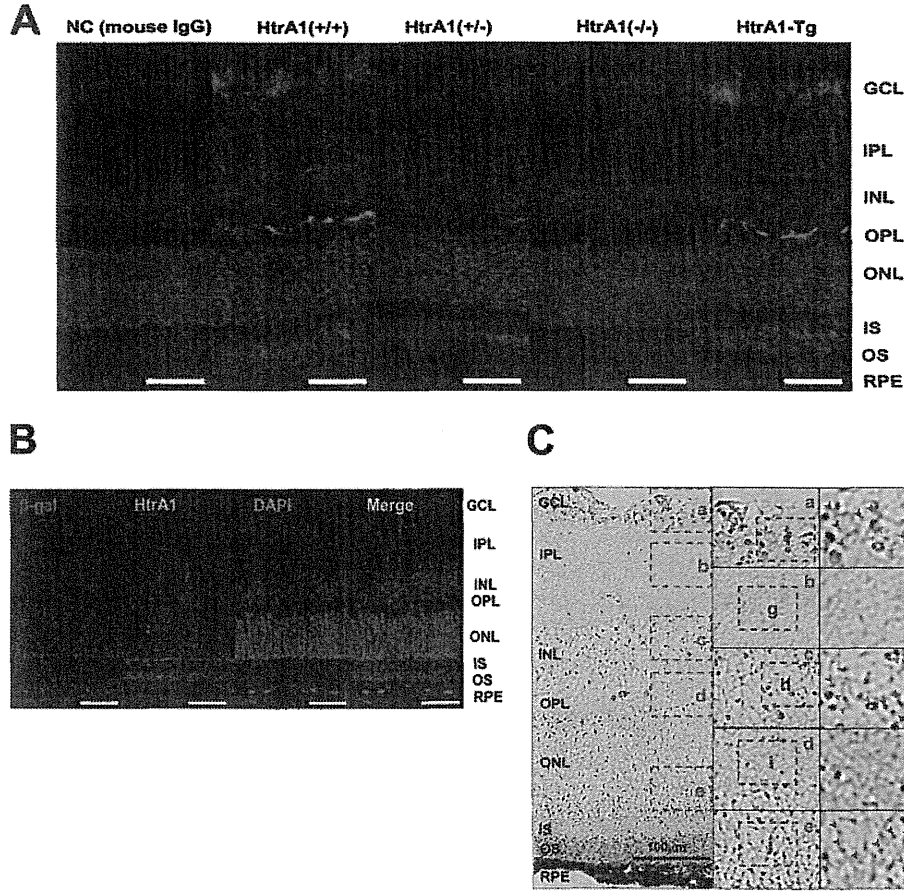

FIGURE 3. ***Htra1* transcription regulator activity and Htra1 protein expression in the mouse retina.** *A*, immunohistochemistry to detect HtrA1 expression in *HtrA1*$^{+/+}$, *HtrA1*$^{+/-}$, *HtrA1*$^{-/-}$, and *HtrA1-Tg* mouse retinas (*blue*, DAPI; *green*, HtrA1). *NC* (mouse IgG), staining control; *scale bars*, 100 μm. *B*, immunohistochemistry to detect HtrA1 expression in *HtrA1*$^{+/-}$ mouse retinas (*red*, β-galactosidase; green: HtrA1; *blue*, DAPI; *yellow*, merge). *Scale bars*, 100 μm. *C*, *in situ* hybridization to detect *HtrA1* expression in *HtrA1*$^{+/-}$ mouse retina tissues (*red arrowheads*, *HtrA1*; *blue arrowheads*, β-galactosidase). *Scale bars*, 100 μm. *OS*, outer segment; *IS*, inner segment; *ONL*, outer nuclear layer; *OPL*, outer plexiform layer; *INL*, inner nuclear layer; *IPL*, inner plexiform layer; *GCL*, ganglion cell layer.

HtrA1 expression was observed to localize to the photoreceptor cell layer (outer segment (*OS*) and inner segment (*IS*) in Fig. 3), the outer plexiform layer (*OPL*), and the ganglion cell layer (*GCL*). In contrast, HtrA1 expression in eye tissues from heterozygous *HtrA1* mice was mainly localized to the photoreceptor cell layer and the outer plexiform layer, whereas minor expression of HtrA1 was observed in the ganglion cell layer.

To localize *HtrA1* transcription regulator activity in the retina, a heterozygous *HtrA1* knock-out mouse construct that included β-galactosidase (β-gal) cDNA (*LacZ*) in place of exon 1 of *Htra1* was used. β-Gal protein was abundantly expressed in the outer nuclear layer (*ONL*), and lower levels of expression were observed in the RPE, the inner nuclear layer (*INL*), and the retinal ganglion cell layer (*GCL*) (Fig. 3*B*). In comparison, native HtrA1 protein was abundantly expressed in the OS and IS, with lower expression levels detected in the RPE, the outer plexiform layer (*OPL*), the inner plexiform layer (*IPL*), and the ganglion cell layer (Fig. 2*B*). Furthermore, abundant transcription of *HtrA1* mRNA was detected by *in situ* hybridization in retinal sections from a *HtrA1* heterozygous knock-out mouse (Fig. 3*C*). Taken together, these results suggest that *HtrA1* is transcribed mainly in the outer nuclear layer, outer plexiform layer, and ganglion cell layer, and then the protein product is transported to the photoreceptor layer.

Identification of Suppressing and Activating cis-Elements in the HTRA1 Regulatory Element—To analyze the mechanism of insertion/deletion function in the *HTRA1* regulatory region, both non-insertion/deletion (*1*, bp −4,320 to +1; *2*, bp −4,238 to +1; *3*, bp −4,022 to +1; *4*, bp −3,936 to +1; *5*, bp −3,777 to +1) and insertion/deletion (*6*, bp −3,936 to +1; *7*, bp −3,854 to +1; *8*, bp −3,788 to +1; *9*, bp −3,836 to −3,788 defect mutant) regions were cloned into a pGL4.10[*luc2*] luciferase assay vector (Fig. 4*A*). These cloned vectors were then transfected into 661W cells and were analyzed for *HTRA1* transcription regulator activity. The activity of the number 2 region (bp −4,320 to −4,239) non-insertion/deletion defect *HTRA1* transcription regulator was 1.8–2-fold higher than that of the number 1 region, and transcription regulator activity did not differ between the number 2, 3, and 4 variants (Fig. 4*B*). In contrast, the activity of the number 5 transcription regulator was 20–30% higher than that of the number 4 variant (Fig. 4*B*).

In addition, activity of the number 6 insertion/deletion type *HTRA1* transcription regulator was 2- and 3-fold higher than that of the number 1 non-insertion/deletion type transcription regulator in 661W cells (Figs. 1*K* and 4*C*). Furthermore, activity

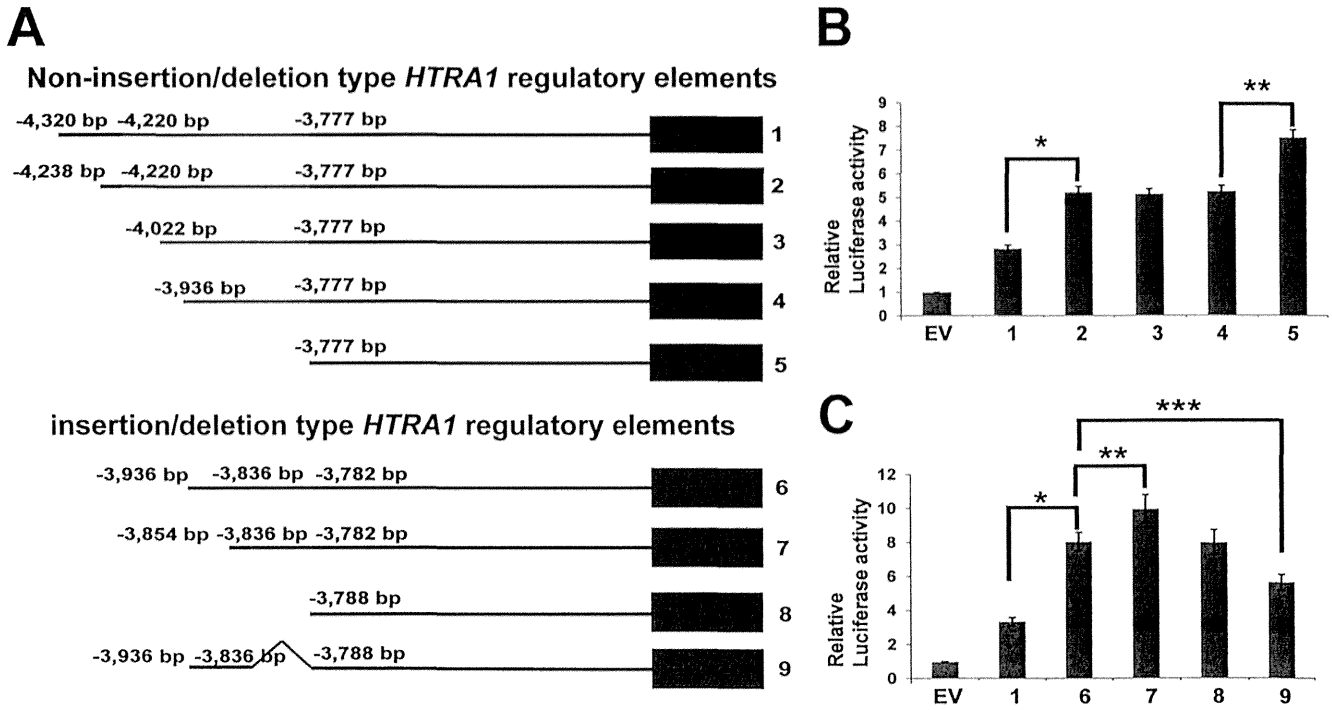

FIGURE 4. **Enhanced *HTRA1* transcription regulator activity is associated with the insertion/deletion variant in the photoreceptor cell line, 661W.** *A*, constructs used for luciferase assay analysis (*black line*, common sequence between both regulators; *blue line*, non-insertion/deletion regulator (443 bp); *red line*, insertion/deletion regulator (54 bp); *red boxes 1–5*, non-insertion/deletion regulator constructs; *green boxes 6–9*, insertion/deletion regulator constructs; *gray line 9*, insertion/deletion region). *B* and *C*, transcription regulator activity detected for the non-insertion/deletion and insertion/deletion *HTRA1* transcription regulator assayed (in *B*, *, $p = 1.05 \times 10^{-6}$; **, $p = 3.46 \times 10^{-5}$; in *C*, *, $p = 2.2 \times 10^{-6}$; **, $p = 0.0086$; ***, $p = 0.0062$). *EV*, empty vector; *error bars*, S.D.

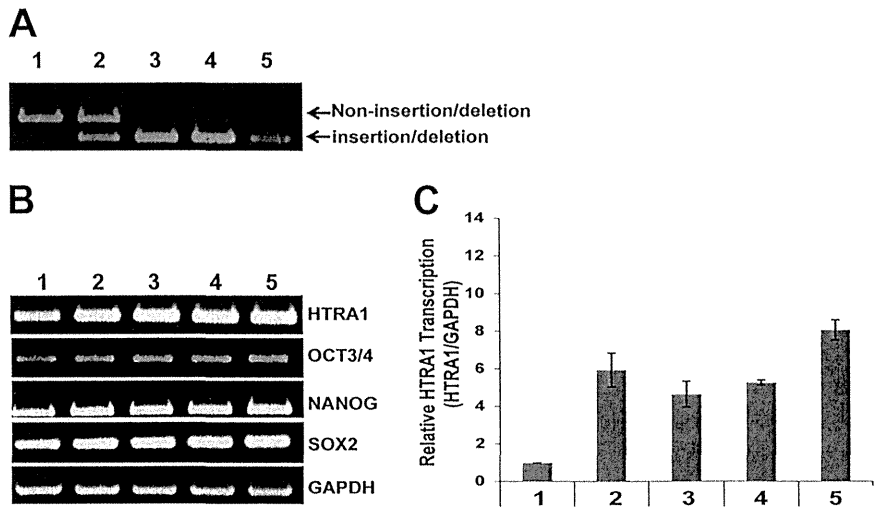

FIGURE 5. **HTRA1 transcription in human iPSCs derived from wet AMD patients.** *A*, genotyping of non-insertion/deletion *versus* insertion/deletion versions of the human *HTRA1* gene transcription regulatory region. *B*, detection of human iPSC marker genes by RT-PCR. Detection of GAPDH was used as an internal control. *C*, relative transcriptional level of *HTRA1* determined by quantitative RT-PCR for iPSCs derived from individuals with non-insertion/deletion (control) *versus* insertion/deletion (wet AMD) transcription regulators. *Sample 1*, 30-year-old non-AMD male; *sample 2*, 72-year-old wet AMD female; *sample 3*, 38-year-old non-AMD male; *sample 4*, 71-year-old non-AMD female; *sample 5*, 71-year-old wet AMD female. *Error bars*, S.D.

of the number 7 (bp −3,936 to −3,855 defect) region was 10% higher than that of the number 6 region, and activity of the number 8 (bp −3,936 to −3,789 defect) region was lower than that of the number 7 region (Fig. 4*C*). In addition, the activity of the number 9 (insertion/deletion defect) region was 10–20% lower than that of the number 6 insertion/deletion type transcription regulator (Fig. 4*C*). Taken together, these results suggest that both of the non-insertion/deletion type regions (including bp −4,320 to −4,239 and bp −3,936 to −3,778 bp) may be regulated by suppressor factors, whereas the insertion/deletion type region from bp −3,836 to −3,789 may bind an enhancer.

Endogenous HTRA1 Expression Is Enhanced by the Insertion/Deletion Type Regulatory Element in AMD Patient iPSCs—To determine the level of *HTRA1* expression in individuals with a non-insertion/deletion type regulatory element sequence,